

Adaptive Perturbation Generation for Multiple Backdoors Detection

Anonymous submission

Abstract

Extensive evidence has demonstrated that deep neural networks (DNNs) are vulnerable to backdoor attacks, which motivates the development of backdoor detection methods. Existing backdoor detection methods are typically tailored for backdoor attacks with individual specific types (*e.g.*, patch-based or perturbation-based). However, adversaries are likely to generate multiple types of backdoor attacks in practice, which challenges the current detection strategies. Based on the fact that adversarial perturbations are highly correlated with trigger patterns, this paper proposes the *Adaptive Perturbation Generation* (APG) framework to detect multiple types of backdoor attacks by adaptively injecting adversarial perturbations. Since different trigger patterns turn out to show highly diverse behaviors under the same adversarial perturbations, we first design the global-to-local strategy to fit the multiple types of backdoor triggers via adjusting the region and budget of attacks. To further increase the efficiency of perturbation injection, we introduce a gradient-guided mask generation strategy to search for the optimal regions for adversarial attacks. Extensive experiments conducted on multiple datasets (CIFAR-10, GTSRB, Tiny-ImageNet) demonstrate that our method outperforms state-of-the-art baselines by large margins (+12%)¹.

1 Introduction

Deep Neural Networks (DNNs) have shown vast potential in various areas (Krizhevsky, Sutskever, and Hinton 2012; He et al. 2016; Devlin et al. 2018). Nowadays, Machine Learning as a Service (MLaaS) platforms have emerged to outsource model training for developers since it often requires high computational resources for training high-quality DNNs. However, there exist strong security issues when using online platforms due to the black-box training process, such as backdoor attack (Gu, Dolan-Gavitt, and Garg 2017) where attackers can embed backdoors into models during training to manipulate model behaviors with specific trigger patterns during inference.

To mitigate the challenges brought by backdoor attacks, a long line of backdoor detection methods have been proposed. However, most of them are tailored for several specific types of backdoor attacks. For example, Guo, Li, and

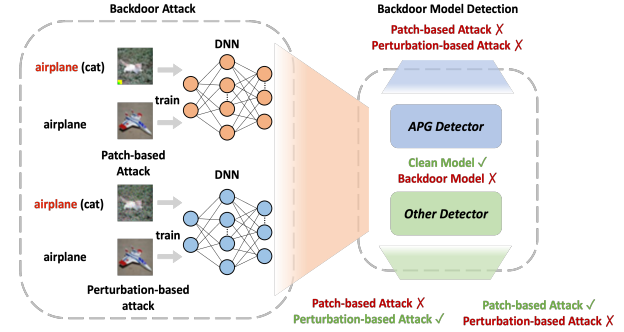


Figure 1: Previous backdoor detection methods are tailored for specific types of backdoor attacks, while our paper focuses on the more practical and challenging scenario to detect multiple types of backdoor poisoned models.

Liu can only detect backdoor attacks with small trigger patterns but show significantly weak performance on backdoor attacks using large trigger patterns. In practice, adversaries are likely to embed multiple types of backdoor attacks containing diversified and stealthy trigger patterns such as invisible (Nguyen and Tran 2021) and sample-specific (Nguyen and Tran 2020), which brings potential challenges to the existing backdoor detection methods.

In this paper, we primarily focus on detecting multiple backdoor attacks with different trigger sizes and trigger transparencies to improve the general detection ability of existing backdoor detections in the more challenging and practical scenario (as shown in Figure 1). Since adversarial perturbations are highly correlated with backdoor trigger patterns (Mu, Wang, and Niu 2022), we propose *Adaptive Perturbation Generation* framework to detect multiple types of backdoor attacks by injecting adversarial perturbations.

The first question is how to inject adversarial perturbations. Different types of trigger patterns with different sizes and transparencies turn out to show highly diverse behaviors under the same adversarial perturbations, we, therefore, design the global-to-local strategy to fit multiple backdoor trigger patterns by adjusting the region and budget of adversarial attacks with adaptive adversarial perturbations. Regarding the perturbation region, we introduce the mask generation strategy to shrink the area of adversarial attacks gradu-

¹Our codes can be found in the supplementary material.

ally; considering the perturbation budget, we build the budget increment measure to search the intensity of adversarial attacks in various pixel spaces to better activate the latent backdoor. One remaining question is that random mask generation requires large-scale region search, which is inefficient and would decrease the overall detection performance. Thus, we further propose the gradient-guided mask generation strategy to search for the optimal area for attacks using adversarial gradient. Finally, based on the observation that adversarial attacks would lure backdoored models in a skewed output distribution towards target labels, we utilize Median Absolute Deviation (MAD) algorithm (Hampel 1974) to help detect the abnormal output distribution and thus identify the backdoored models. Extensive experiments are conducted on CIFAR-10, GTSRB, and Tiny-ImageNet, which demonstrate that our APG achieves promising performance on detecting multiple backdoor attacks and outperforms existing detection strategies by large margins (**+12%**). Our **contributions** are summarized as follows:

- Based on the fact that adversarial perturbations are highly correlated to trigger patterns, we propose the *Adaptive Perturbation Generation* (APG) framework to detect multiple types of backdoor attacks.
- We implement a global-to-local approach to search for the attack region and attack budget for simulating different trigger sizes and transparencies. Furthermore, we design the gradient-guided strategy to improve the perturbation region search efficiency.
- Extensive experiments on various datasets demonstrate that our detection framework can achieve promising detection accuracy on multiple backdoor attacks, and outperforms others by large margins.

2 Related Work

Backdoor Attack

Backdoor attack mainly affects the training process and forces a mapping between trigger pattern and target label. The backdoored model will show malicious behavior when the input image tampers with a trigger. Otherwise, it will behave normally. Gu, Dolan-Gavitt, and Garg first proposed BadNets by sticking a patch-based trigger on the training data and changing their labels to a specific target class (dirty-label attack). Then, some works were proposed to improve backdoor injection. Liu et al. optimized the trigger pattern and implemented the backdoor attack using transfer learning, Nguyen and Tran designed both a mask and trigger generator to generate sample-specific triggers.

However, the patch-based trigger can be detected by humans easily which motivates some researches on more stealthy backdoor attacks. Chen et al. poisoned the training dataset with a global pattern and increased trigger transparency to evade human inspection. Nguyen and Tran utilized image wrapping to make the poisoned natural-looking. While dirty label attacks are easily detected, other attacks (Turner, Tsipras, and Madry 2019; Barni, Kallas, and Tondi 2019; Saha, Subramanya, and Pirsivash 2020; Zhao et al. 2020) only poisoned the data in the target class without

changing the original label (clean-label attack) which increased the stealthiness of the backdoor attack.

Backdoor Detection

To mitigate the impact of backdoor attacks, many detection methods have been proposed. Typically, the existence of backdoor attack can be detected in the training set (Tran, Li, and Madry 2018; Gao et al. 2019) as well as the trained model (Wang et al. 2019). In this paper, without access to the original training set, we only consider conducting the backdoor detection on the models after training, which is more practical. Neural Cleanse (Wang et al. 2019) first identified the shortcut hidden in the backdoor models and detected the latent backdoor based on trigger reconstruction. The following work (Guo et al. 2020; Wang et al. 2020) improved Neural Cleanse with better detection accuracy, and others like (Zhu et al. 2020; Qiao, Yang, and Li 2019) made use of the generative adversarial network (GAN) to recover the trigger. Some work even focused on black-box setting (Guo, Li, and Liu 2021) with only hard output label and distinguished backdoor models using peak value in adversarial maps. However, these methods are less effective in detecting large triggers. Recently, studies (Kolouri et al. 2020; Xu et al. 2021) also used extra classifiers to detect different types of backdoor models but they still fail against attacks that do not appear in the training set.

To sum up, in contrast all previous studies that primarily focus on specific types of backdoor attacks, our proposed APG framework aims to detect multiple types of backdoor attacks with different trigger sizes and transparencies.

Adversarial Attack

Adversarial attacks are inputs intentionally designed to mislead deep learning models during inference but are imperceptible to humans (Szegedy et al. 2013; Goodfellow, Shlens, and Szegedy 2014). A long line of work has been proposed to attack deep learning models (Goodfellow, Shlens, and Szegedy 2014; Kurakin, Goodfellow, and Bengio 2018; Liu et al. 2019, 2020), which can be roughly divided into white-box attacks and black-box attacks depending on the access to the target model. In this paper, we use adversarial attacks to help diagnose whether the model is embedded with backdoor attacks.

3 Methodology

The APG framework is introduced in this section. We first define the backdoor attack and backdoor detection task. Then, we describe our framework overview, followed by a detailed introduction and the overall detecting process.

3.1 Problem Definition

Backdoor Attack cheats models through embedding triggers to benign input during training phase. Considering the trigger patterns, we divide backdoor attacks into patched-based and perturbation-based categories. For patch-based backdoor attacks, the general injection function is :

$$\hat{\mathbf{x}} = (1 - \mathbf{m}) \odot \mathbf{x} + \mathbf{x} \odot \Delta,$$

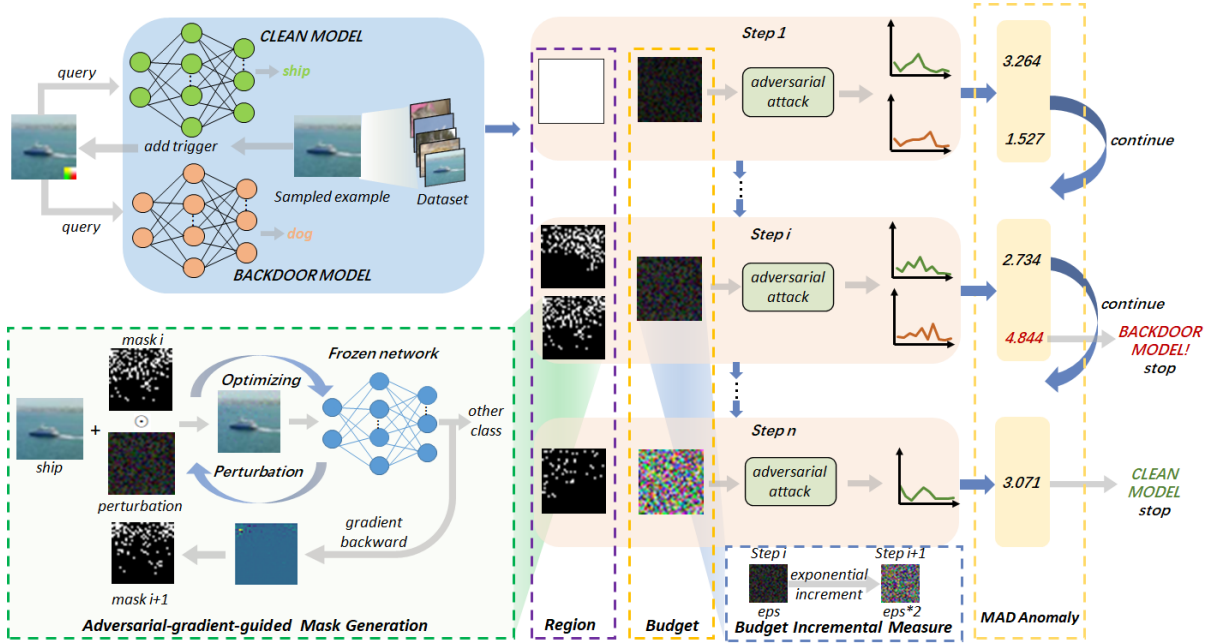


Figure 2: The overview of the proposed APG framework. We dynamically search the optimal perturbation by adjusting the region and budget through gradient-guided mask generation strategy and budget increment measure. The goal of APG is detecting multiple types of backdoor attacks.

where $\Delta \in R^{w \times h \times c}$ represents the backdoor trigger and \odot represents the element-wise product. $m \in \{0, 1\}^{w \times h}$ is a binary mask that ensures the position and magnitude of the backdoor trigger. For perturbation-based backdoor attacks, the general injection function is:

$$\hat{\mathbf{x}} = \mathbf{x} + t \odot \Delta,$$

where $t \in \mathbb{R}$ represents the transparency of trigger. The patch-based backdoor triggers are usually in patch shape with small $\|m\|_1$, while the perturbation-based backdoor triggers are distributed in the whole image with human-imperceptible visibility to ensure stealthiness.

Adversarial Attack cheats the DNN by generating the perturbation δ and superimposing δ on the input, which causes misclassification in DNNs. The optimization objective can be formulated as:

$$\arg \max_{\delta} \sum_n \ell(f(\mathbf{x} + \delta), y),$$

where δ is the adversarial perturbation, n is the number of samples and y is the label of input \mathbf{x} .

Notably, the adversarial attack is mainly an attack in the inference phase, while the backdoor attack is an attack in the training phase.

Backdoor Detection aims to determine whether the model is infected or not. Previous work (Wang et al. 2019; Dong et al. 2021; Chen et al. 2019) use the following optimization to detect backdoor for each target label y_t :

$$\arg \min_{\mathbf{m}, \Delta} \sum_n \ell(\phi((1 - \mathbf{m}) \odot \mathbf{x} + \mathbf{m} \odot \Delta), y) + \beta \|\mathbf{m}\|_1,$$

where β controls the trade-off between mask size and misclassification rate of clean images.

3.2 Framework Overview

General backdoor detection methods usually focus on specific backdoor attacks while are not applicable for other backdoor attacks. Thus, we aim to implement a unified backdoor detection approach to detect multiple backdoor attacks. Previous work (Mu, Wang, and Niu 2022) reveals adversarial perturbations are highly correlated with backdoor trigger patterns, which demonstrates that it is feasible to fit backdoor triggers with adversarial perturbations. Therefore, we propose the APG framework to fit various backdoor trigger patterns for multiple backdoors detection. Figure 2 shows the overall framework of APG.

We first design the global-to-local approach, which searches for optimal adversarial perturbations by adjusting the region and budget dynamically. For the region, we implement the mask generation strategy to shrink the area of adversarial attacks gradually. For the budget, we utilize an incremental measure to search the intensity of adversarial attacks to activate the latent backdoor better. One remaining question is that random mask generation requires large-scale region search, which motivates us to propose gradient-guided mask generation strategy. Since the adversarial gradient reflects the degree of influence on adversarial attacks, we can thus shrink the region by selecting a certain proportion of pixels with larger adversarial gradients, which can be regarded as better attacking regions.

3.3 Global-to-Local Approach

Fitting different trigger patterns through adversarial perturbations, we achieve the global-to-local approach. Specifically, we consider trigger patterns in terms of trigger size and

trigger transparency, which motivates us to generate adversarial perturbations from both region and budget. Therefore, the global-to-local approach consists of two parts: mask generation strategy and budget increment measure.

Mask Generation Strategy

The mask generation strategy is designed to search for an optimal region for adversarial attacks because of the potential differences between the backdoor attacks with different trigger patterns. We deem that trigger size is a critical parameter embedded in the DNNs. In fact, patch-based triggers will guide DNNs to focus on local areas, while perturbation-based is evenly and regularly distributed in the global areas. Based on this phenomenon, we introduce our mask generation strategy.

Specifically, given a sample \mathbf{x} , we generate the corresponding mask \mathbf{m}_i at each stage i to shrink the region, which could be formulated as:

$$m_i^k = \begin{cases} 1, & \rho \leq \alpha_i, \\ 0, & \rho > \alpha_i. \end{cases}$$

where m_i^k is the k -th binary element of mask \mathbf{m}_i . ρ is random variable ($\rho \sim U(0, 1)$) and $\alpha_i \in (0, 1]$ is selection ratio which could be formulated as:

$$\alpha_i = \alpha_{i-1} - \eta,$$

where $\eta \in (0, 1)$ represents a constant that decreases with each step.

In summary, we search for the optimal region of adversarial attack by mask generation strategy. We first generate a global perturbation ($\alpha_1 = 1$) to simulate perturbation-based trigger, then start from the perturbation of 25% ($\alpha_i = 0.25$) of the whole image, and gradually shrink the region step by step until region is less than 1% ($\alpha_i \leq 0.01$) of the whole image, adapting various trigger sizes in the most existing patch-based backdoor attack approaches.

Budget Increment Measure

Except for the attack region, we further notice that the magnitude of adversarial perturbations controlled by ϵ -ball constraint also influences the activation of backdoor DNNs. To explore the similarity between trigger transparencies and attack budget, we generate two perturbations within both large ϵ -ball and small ϵ -ball constraint, respectively, and observe that perturbations with visual similarity to triggers that can activate the latent backdoor.

Based on our observation, we deem that the magnitude constraint, defined as budget, can simulate the trigger transparency. By utilizing the ϵ -ball constraint, we increase the budget for each step as:

$$\mathcal{B}_i = \max(\mathcal{B}_{i-1} \times 2, 1),$$

where $\mathcal{B} \in [8/255, 1]$ represents the budget in the i -th step. For simplicity, we use exponentially incremental measure by the factor 2. We also try other incremental measures, such as adding a constant and find that exponential increment is better in terms of detection performance. This is reasonable since we find adversarial perturbations with the

large region and high budget activate specific neurons rather than the latent backdoor, which will mislead backdoor detection. As we further shrink the region, we simulate the patch-based trigger in a smaller region with a higher attack budget. Therefore we avoid adopting a high budget in the first few steps and increase the attack budget exponentially.

3.4 Gradient-Guided Mask Generation Strategy

Based on the global-to-local strategy, we can well fit various backdoor trigger patterns to achieve multiple backdoors detection. However, one remaining question is that random mask generation requires large-scale region search, which is inefficient and would decrease the overall detecting performance. Therefore, we further propose the gradient-guided strategy to search for the optimal region area for adversarial attacks using the adversarial gradient.

By utilizing the softmax outputs to calculate the anomaly index, it is critical to ensure sufficient samples. We observe the average anomaly index in backdoor models under different samples per class, demonstrating that sufficient samples can improve the performance of backdoor detection. Specifically, it is detrimental to backdoor detection with insufficient attacked samples, which is reasonable because some samples are inherently vulnerable to adversarial attacks, reducing the chance of activating latent backdoor tendency. Actually, under the same conditions, the number of attacked samples is based on the attack success rate(ASR) of adversarial attacks, which demonstrates that backdoor detection performance is better in the adversarial attack under high ASR. Therefore, we aim to find the sensitive pixels that most mitigate the drop in ASR when we shrink the region for adversarial attacks.

Generating perturbations for backdoor detection by the adversarial attack, we can reasonably choose the adversarial gradient to select regions for the next detection step, which motivates us to propose the *gradient-guided* mask generation. We demonstrate that as the region size decreases, the ASR of adversarial attack also decreases and decreases more on the random mask generation than *gradient-guided* mask generation. The *gradient-guided* mask generation strategy can be formulated as:

$$\mathbf{m}_i = \text{Top}_{\alpha_{i-1}}(\nabla_{\mathbf{x}_{\text{adv}}} L(f(\mathbf{x}_{\text{adv}}, \theta)))$$

where α is the proportion of reduced area in the whole map and X_{adv} is the adversarial samples. For each image, we generate the sample-specific mask for it.

3.5 Overall Detecting Process

In our proposed approach, we adaptively fit different backdoor trigger patterns via adjusting the region and budget of the adversarial attack. After injecting the adversarial perturbations generated by optimal region and budget, we utilize the MAD algorithm to help detect the abnormal output distribution and thus identify the backdoored model.

Specifically, for each sample \mathbf{x} , we set the initial region and budget for adversarial attack to the whole image and 8/255 respectively. We then generate perturbation for each sample \mathbf{x} through several attack iterations. The perturbation

generated by APG in each attack iteration j is:

$$\mu_j = \varepsilon * \text{sign}(\nabla_{\mathbf{x}_j \odot \mathbf{m}_i} L(f(\mathbf{x}_j; \theta), y_t)),$$

where \mathbf{m}_i is the mask for step i and we only generate the adversarial perturbation in the mask region. We then limit the perturbation within the attack budget \mathcal{B} as:

$$\mathbf{x}_j = \Pi_{\mathbf{x} + \mathcal{B}_i} (\mathbf{x}_{j-1} \odot (1 - \mathbf{m}_i) + (\mathbf{x}_{j-1} \odot \mathbf{m}_i + \mu_{j-1})),$$

after several attack iterations, we finally obtain the adversarial samples with masked perturbations. We then calculate the softmax outputs of attacked samples and utilize MAD to detect the outliers. We identify the model as an backdoored model if anomaly index is larger than threshold. We iteratively conduct APG and terminate when the model is identified as an backdoored model or the budget is up to 1.

More details of our proposed APG could be found in the supplementary material.

4 Experiments

4.1 Experimental Setups

Datasets and Architectures In this paper, we evaluate our methods on image classification tasks using CIFAR-10 (Krizhevsky, Hinton et al. 2009), GTSRB (Stallkamp et al. 2012), and Tiny-ImageNet (Le and Yang 2015). For model architectures, we use ResNet-18 (He et al. 2016), VGG19 (Simonyan and Zisserman 2014), DenseNet-161 (Huang et al. 2017), and MobileNet-V2 (Sandler et al. 2018). For each backdoor attack, we build 60 infected models and 60 benign models evenly distributed over the four architectures on each dataset. We randomly select one target label for each infected model and inject around 10% poisoned samples into training data making the average attack success rate $\geq 90\%$.

Backdoor Attack We choose four backdoor attacks with different trigger patterns to evaluate APG including BadNets (Gu, Dolan-Gavitt, and Garg 2017), Blend (Chen et al. 2017), WaNet (Nguyen and Tran 2021), and Input-Aware (Nguyen and Tran 2020). For BadNets, we use two triggers patterns, namely the small scale squares (BadNets-s) and the large scale squares (BadNets-l); for Blend, we use both the Gaussian Noise pattern and Hello Kitty pattern, and the transparency ratios are 0.9 (Blend-l) and 0.95 (Blend-h); for WaNet and Input-Aware, we use the default settings following the previous work. It is worth noting that Input-Aware is a sample-specific backdoor attack method which challenges existing backdoor detection methods.

Detection baselines We compare APG with the state-of-the-art backdoor detection methods Neural Cleanse (NC) (Wang et al. 2019) and DF-TND (Wang et al. 2020). Specifically, for each dataset, we randomly select 40 test samples evenly from each class to generate adversarial perturbations.

Implementation Details For adversarial attacks, we utilize the commonly-used PGD (Madry et al. 2017) to perform white-box untargeted attacks. We take 40 steps to optimize adversarial perturbations and set step size to 0.001. For our MAD detector, we set the threshold as $\tau = 3.5$ for CIFAR-10, and adaptively increase according to categories.

Evaluation Metrics Following (Kolouri et al. 2020), we use *The Area under Receiver Operating Curve* (AUROC) and

Detection Accuracy (ACC) to evaluate the detection performance on specific types of attacks; we also report *Average Attacks* to calculate the average detection ACC on several types of backdoor attacks. For each metric, a higher value means the better performance of backdoor detection.

We defer more details of our experimental setups in the supplementary material.

4.2 Comparison with Other Baselines

In this section, we compare APG with other backdoor detection methods. As shown in Table 1, our APG framework achieves significantly higher values on *Average Attacks* than other baselines in general. In particular, our performance is obviously better than other methods under some specific trigger patterns (*i.e.*, large-size trigger and high-transparency trigger) and is overall robust across different attack methods and datasets. We make several conclusions as follows.

(1) For patch-based backdoor attacks (BadNets), APG and DF-TND exhibit a stable detection ability despite the trigger sizes, while NC turns out to show weak performance on BadNets-l. We attribute this to the particular searching strategy of APG, which can well fit backdoor triggers with different sizes. We also notice that as the number of classes increases (200 classes in Tiny-ImageNet), the detection accuracy of infected labels degrades, which causes the less robustness of all three methods.

(2) For perturbation-based backdoor attacks (Blend), APG achieves higher ACC and AUROC than other detection methods across three different datasets. We also notice that APG is robust to perturbation-based trigger with different transparencies and achieves an overall detection accuracy over 99%. We further explore the detection stability of APG with different trigger transparencies in later experiments.

(3) For Input-Aware attack, we can see the detection ACC is related to the dataset, and our proposed APG performs well on GTSRB. We believe this is because Input-Aware generates specific perturbation for each sample, perturbing the space to activate latent backdoor.

(4) To better illustrate the general detection performance over the four backdoor attacks, we list the *Average Attacks* of three datasets, respectively. The *Average Attacks* demonstrate that APG exhibits robustness across different dataset and attack methods which outperforms an average of **+12%** *Average Attacks* against other two detection methods.

(5) Apart from the ACC, we also observe that the overall AUROC of APG is higher than the other two detection methods with an average value of **0.958**. Such experimental results demonstrate that the high backdoor ACC of APG does not sacrifice the ACC of clean models. Therefore, APG is much more robust than existing detection methods.

To sum up, APG achieves the best performance compared to existing backdoor detection approaches on multiple backdoor attacks across different settings, especially in some complex scenarios (*e.g.*, hardly-inspected perturbation-based backdoor attack).

Table 1: Detection results (ACC, AUROC) on each dataset using three backdoor detection methods: NC, DF-TND and APG. Average Attacks measures the average detection performance on all backdoor attacks. Higher values in all metrics are better. Each approach are evaluated using 60 infected and 60 benign models in a task.

Attack	Method	Detection Results						
		CIFAR-10		GTSRB		Tiny-ImageNet		
		ACC(%)	AUROC	ACC(%)	AUROC	ACC(%)	AUROC	
BadNets	-s	NC	90.000	0.945	100.00	0.978	63.333	0.851
		DF-TND	98.333	0.999	100.00	1.000	78.333	0.885
		APG (Ours)	96.667	0.986	98.333	0.998	73.333	0.879
	-l	NC	73.333	0.865	91.667	0.949	18.333	0.403
		DF-TND	91.667	0.974	90.000	0.971	41.667	0.732
		APG (Ours)	93.333	0.976	93.333	0.992	48.333	0.742
Blend	-h	NC	58.333	0.834	93.333	0.961	80.000	0.936
		DF-TND	56.667	0.799	58.333	0.784	51.667	0.792
		APG (Ours)	98.333	0.995	100.00	1.000	98.333	0.978
	-l	NC	96.667	0.981	91.667	0.958	96.667	0.986
WaNet	DF-TND	58.333	0.801	61.667	0.809	50.000	0.679	
	APG (Ours)	98.333	0.990	100.00	1.000	100.00	0.991	
	NC	86.667	0.910	40.000	0.711	71.667	0.874	
Input-aware	DF-TND	66.667	0.825	63.333	0.815	68.333	0.841	
	APG (Ours)	90.000	0.969	88.333	0.989	78.333	0.929	
	NC	20.000	0.531	66.667	0.878	6.6667	0.630	
Average Attacks	DF-TND	43.333	0.681	60.000	0.843	18.333	0.638	
	APG (Ours)	36.667	0.830	74.000	0.968	13.333	0.691	
	NC	70.833	0.844	80.556	0.906	56.111	0.780	
Average Attacks	DF-TND	69.167	0.847	72.222	0.870	51.389	0.761	
	APG (Ours)	85.556	0.958	92.333	0.991	68.611	0.868	

4.3 Detection on More Rigorous Scenarios

In this section, we further investigate the detection performance of APG on more rigorous scenarios with various trigger sizes and transparencies.

Different Trigger Sizes For simplicity, we utilize white squares with different sizes (from 2×2 to 14×14) and train 24 infected models for each size on CIFAR-10 with ResNet-18. Figure 3(a) illustrates that the ACC of NC decreases significantly and shows less robustness as the trigger size is larger than 12×12 . However, DF-TND and APG remain effective with $ACC \geq 62.5\%$ even if the trigger size expands to the exaggerated size 14×14 which takes around 20% of the whole image. This demonstrates that APG and DF-TND are robust to trigger with various sizes. We also notice that except for the 14×14 trigger, the ACC of our APG is slightly better than that of DF-TND.

Different Trigger Transparencies We then evaluate APG on CIFAR-10 with different trigger transparencies (from 0.7 to 0.95) using Blend attack. For each trigger transparency, we train 24 infected models with ResNet-18. Figure 3(b) shows that APG remains effective against all trigger transparencies with $ACC \geq 66.67\%$, while NC and DF-TND perform worse when trigger transparency is too high (0.95) or too low (0.7). The results demonstrate that the performance of APG is robust to trigger transparency.

4.4 Ablation Studies

In this section, we further ablate the influence of the critical factors in our proposed APG framework, *i.e.* different mask

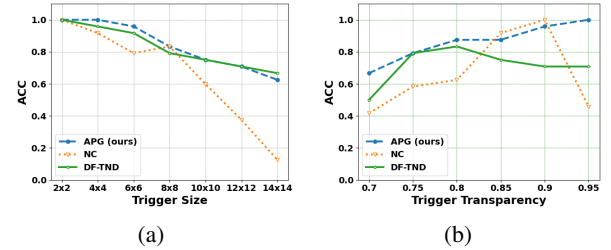


Figure 3: The impact of trigger pattern among three detection methods. (a) The impact of trigger sizes on ACC. (b) The impact of trigger transparencies on ACC.

generation strategies.

The Impact of Mask Generation Strategy We evaluate two kinds of mask generation strategies (random and gradient-guided) using 40 ResNet-18 BadNets models trained on poisoned CIFAR-10 dataset (4×4 white square). Figure 4(a) shows the gradient-guided strategy has higher ACC in early detection steps, which is much more efficient than random mask generation strategy. We attribute this superiority to the fact that the gradient-guided mask generation strategy can better maintain ASR for adversarial attacks. We further prove our conjecture by computing ASR using two mask generation strategies. The results shown in Figure 4(b) illustrate that gradient-guided mask generation provides high ASR despite attack budget.

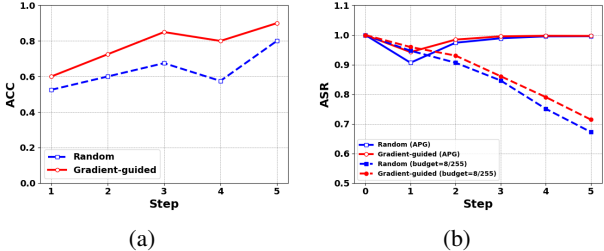


Figure 4: Comparison between random and gradient-guided mask generation strategy. (a) Detection ACC on each step on two mask generation strategies. (b) The changing law of ASR under two mask generation strategies.

We defer more details of our ablation studies in the supplementary material.

4.5 Analysis and Discussion

In this section, we provide more studies and analyses to better understand our APG framework.

Relationship between Adversarial Perturbations and Backdoor Triggers

To better understand the effectiveness of adaptive attacking approach, we hereby conduct experiments on CIFAR-10 to reveal the relationship between adversarial perturbations and backdoor triggers in terms of attack regions and budget. Specifically, we select 10 clean models, 10 BadNets models (4×4 square with complex color on the bottom right corner) and 10 Blend models (Global Gaussian Noise) trained with ResNet-18.

Attack region. We select five square regions (from 2×2 to 32×32) to perform PGD attack with the budget of $8/255$. Figure 5(a) illustrates that the latent backdoor is gradually activated in Blend models as the region size increases. Specifically, this activation on Blend models can be easily detected when region size is larger than 16×16 , but is less significant when region size is small. However, the anomaly index of BadNets models remains relatively stable despite of region size and is similar to clean models. To find a more intrinsical relation, we then investigate the impact of the budget.

Attack budget. We choose six budgets ranging from $2/255$ to $64/255$ to study the impact of budget within a patch region (8×8) on the bottom right corner, and observe the change of the anomaly index under different perturbation budgets. As shown in Figure 5(b), we observe that the latent backdoor of BadNets models is gradually activated as the budget increases. We then combine with our previous study in attack region and further conclude that activation of BadNets models can be achieved by adversarial perturbation with a small region and large budget. Interestingly, we find that perturbations with small regions can also activate the latent backdoor of the blend models, and we leave this problem to our future work.

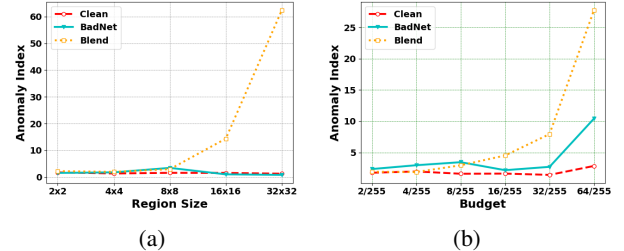


Figure 5: Relationship between adversarial perturbations and backdoor triggers. (a) Analysis of attack region. (b) Analysis of attack budget.

Table 2: Comparison of computational overhead (img/s).

Dataset	NC	DF-TND	APG(Ours)
CIFAR-10	5.76	1.04	10.85
GTSRB	3.38	1.23	12.32
Tiny-ImageNet	0.38	0.36	10.19

Computational Overhead

We examine the computational overhead of APG and other baselines by running all three methods with a single 80GB memory NVIDIA Tesla A100 GPU. Specifically, for each dataset (CIFAR-10, GTSRB, and Tiny-ImageNet), we train 10 ResNet-18 models (5 infected and 5 uninfected) and compute the average running time in seconds for all methods. For NC and APG, we select 40 samples evenly distributed in the classes from each dataset. For DF-TND, we choose 50 samples for CIFAR-10, 150 samples for GTSRB and 200 samples for Tiny-ImageNet. To make a fair comparison, we divide the number of samples by the average time.

We show the results in Table 2, which demonstrates that APG is much faster than NC and DF-TND over all datasets, especially achieving at most 27 times faster in Tiny-ImageNet. The intrinsic reason is that APG utilizes the untargeted adversarial attack, meaning the total time is not easily affected by the number of categories. In comparison, NC and DF-TND examine all labels individually, which takes a massive time as the number of classes increases.

5 Conclusion

In this paper, we propose *Adaptive Perturbation Generation* (APG) framework to achieve multiple types of backdoors detection. In practice, we first design a global-to-local strategy to fit different trigger patterns by adaptively adjusting the region and budget of adversarial perturbation. We then propose the gradient-guided mask generation strategy to help efficiently search for the optimal attack areas. Extensive experiments demonstrate that our APG framework outperforms other comparisons by large margins, *i.e.*, at least **+12%** on Average Attacks. We hope our work will guide future studies on backdoor detection to focus on more complex and multiple backdoor trigger patterns.

In the future, we are interested in searching for optimal perturbation more efficiently and detecting more types of backdoor attacks (*e.g.*, sample-specific attacks).

References

Barni, M.; Kallas, K.; and Tondi, B. 2019. A new backdoor attack in cnns by training set corruption without label poisoning. In *2019 IEEE International Conference on Image Processing (ICIP)*, 101–105. IEEE.

Chen, H.; Fu, C.; Zhao, J.; and Koushanfar, F. 2019. DeepInspect: A Black-box Trojan Detection and Mitigation Framework for Deep Neural Networks. In *IJCAI*, volume 2, 8.

Chen, X.; Liu, C.; Li, B.; Lu, K.; and Song, D. 2017. Targeted backdoor attacks on deep learning systems using data poisoning. *arXiv preprint arXiv:1712.05526*.

Devlin, J.; Chang, M.-W.; Lee, K.; and Toutanova, K. 2018. Bert: Pre-training of deep bidirectional transformers for language understanding. *arXiv preprint arXiv:1810.04805*.

Dong, Y.; Yang, X.; Deng, Z.; Pang, T.; Xiao, Z.; Su, H.; and Zhu, J. 2021. Black-Box Detection of Backdoor Attacks With Limited Information and Data. In *Proceedings of the IEEE/CVF International Conference on Computer Vision (ICCV)*, 16482–16491.

Gao, Y.; Xu, C.; Wang, D.; Chen, S.; Ranasinghe, D. C.; and Nepal, S. 2019. Strip: A defence against trojan attacks on deep neural networks. In *Proceedings of the 35th Annual Computer Security Applications Conference*, 113–125.

Goodfellow, I. J.; Shlens, J.; and Szegedy, C. 2014. Explaining and harnessing adversarial examples. *arXiv preprint arXiv:1412.6572*.

Gu, T.; Dolan-Gavitt, B.; and Garg, S. 2017. Badnets: Identifying vulnerabilities in the machine learning model supply chain. *arXiv preprint arXiv:1708.06733*.

Guo, J.; Li, A.; and Liu, C. 2021. Aeva: Black-box backdoor detection using adversarial extreme value analysis. *arXiv preprint arXiv:2110.14880*.

Guo, W.; Wang, L.; Xu, Y.; Xing, X.; Du, M.; and Song, D. 2020. Towards inspecting and eliminating trojan backdoors in deep neural networks. In *2020 IEEE International Conference on Data Mining (ICDM)*, 162–171. IEEE.

Hampel, F. R. 1974. The influence curve and its role in robust estimation. *Journal of the american statistical association*, 69(346): 383–393.

He, K.; Zhang, X.; Ren, S.; and Sun, J. 2016. Deep residual learning for image recognition. In *Proceedings of the IEEE conference on computer vision and pattern recognition*, 770–778.

Huang, G.; Liu, Z.; Van Der Maaten, L.; and Weinberger, K. Q. 2017. Densely connected convolutional networks. In *Proceedings of the IEEE conference on computer vision and pattern recognition*, 4700–4708.

Kolouri, S.; Saha, A.; Pirsiavash, H.; and Hoffmann, H. 2020. Universal litmus patterns: Revealing backdoor attacks in cnns. In *Proceedings of the IEEE/CVF Conference on Computer Vision and Pattern Recognition*, 301–310.

Krizhevsky, A.; Hinton, G.; et al. 2009. Learning multiple layers of features from tiny images.

Krizhevsky, A.; Sutskever, I.; and Hinton, G. E. 2012. Imagenet classification with deep convolutional neural networks. *Advances in neural information processing systems*, 25.

Kurakin, A.; Goodfellow, I. J.; and Bengio, S. 2018. Adversarial examples in the physical world. In *Artificial intelligence safety and security*, 99–112. Chapman and Hall/CRC.

Le, Y.; and Yang, X. 2015. Tiny imagenet visual recognition challenge. *CS 231N*, 7(7): 3.

Liu, A.; Huang, T.; Liu, X.; Xu, Y.; Ma, Y.; Chen, X.; Maybank, S. J.; and Tao, D. 2020. Spatiotemporal attacks for embodied agents. In *European Conference on Computer Vision*, 122–138. Springer.

Liu, A.; Liu, X.; Fan, J.; Ma, Y.; Zhang, A.; Xie, H.; and Tao, D. 2019. Perceptual-sensitive gan for generating adversarial patches. In *Proceedings of the AAAI conference on artificial intelligence*, volume 33, 1028–1035.

Liu, Y.; Ma, S.; Aafer, Y.; Lee, W.-C.; Zhai, J.; Wang, W.; and Zhang, X. 2017. Trojaning attack on neural networks.

Madry, A.; Makelov, A.; Schmidt, L.; Tsipras, D.; and Vladu, A. 2017. Towards deep learning models resistant to adversarial attacks. *arXiv preprint arXiv:1706.06083*.

Mu, B.; Wang, L.; and Niu, Z. 2022. Adversarial Fine-tuning for Backdoor Defense: Connect Adversarial Examples to Triggered Samples. *arXiv preprint arXiv:2202.06312*.

Nguyen, A.; and Tran, A. 2021. WaNet—Imperceptible Warping-based Backdoor Attack. *arXiv preprint arXiv:2102.10369*.

Nguyen, T. A.; and Tran, A. 2020. Input-aware dynamic backdoor attack. *Advances in Neural Information Processing Systems*, 33: 3454–3464.

Qiao, X.; Yang, Y.; and Li, H. 2019. Defending neural backdoors via generative distribution modeling. *Advances in neural information processing systems*, 32.

Saha, A.; Subramanya, A.; and Pirsiavash, H. 2020. Hidden trigger backdoor attacks. In *Proceedings of the AAAI conference on artificial intelligence*, volume 34, 11957–11965.

Sandler, M.; Howard, A.; Zhu, M.; Zhmoginov, A.; and Chen, L.-C. 2018. Mobilenetv2: Inverted residuals and linear bottlenecks. In *Proceedings of the IEEE conference on computer vision and pattern recognition*, 4510–4520.

Simonyan, K.; and Zisserman, A. 2014. Very deep convolutional networks for large-scale image recognition. *arXiv preprint arXiv:1409.1556*.

Stallkamp, J.; Schlipsing, M.; Salmen, J.; and Igel, C. 2012. Man vs. computer: Benchmarking machine learning algorithms for traffic sign recognition. *Neural networks*, 32: 323–332.

Szegedy, C.; Zaremba, W.; Sutskever, I.; Bruna, J.; Erhan, D.; Goodfellow, I.; and Fergus, R. 2013. Intriguing properties of neural networks. *arXiv preprint arXiv:1312.6199*.

Tran, B.; Li, J.; and Madry, A. 2018. Spectral signatures in backdoor attacks. *Advances in neural information processing systems*, 31.

Turner, A.; Tsipras, D.; and Madry, A. 2019. Label-consistent backdoor attacks. *arXiv preprint arXiv:1912.02771*.

Wang, B.; Yao, Y.; Shan, S.; Li, H.; Viswanath, B.; Zheng, H.; and Zhao, B. Y. 2019. Neural cleanse: Identifying and mitigating backdoor attacks in neural networks. In *2019 IEEE Symposium on Security and Privacy (SP)*, 707–723. IEEE.

Wang, R.; Zhang, G.; Liu, S.; Chen, P.-Y.; Xiong, J.; and Wang, M. 2020. Practical detection of trojan neural networks: Data-limited and data-free cases. In *European Conference on Computer Vision*, 222–238. Springer.

Xu, X.; Wang, Q.; Li, H.; Borisov, N.; Gunter, C. A.; and Li, B. 2021. Detecting ai trojans using meta neural analysis. In *2021 IEEE Symposium on Security and Privacy (SP)*, 103–120. IEEE.

Zhao, S.; Ma, X.; Zheng, X.; Bailey, J.; Chen, J.; and Jiang, Y.-G. 2020. Clean-label backdoor attacks on video recognition models. In *Proceedings of the IEEE/CVF Conference on Computer Vision and Pattern Recognition*, 14443–14452.

Zhu, L.; Ning, R.; Wang, C.; Xin, C.; and Wu, H. 2020. Gangsweep: Sweep out neural backdoors by gan. In *Proceedings of the 28th ACM International Conference on Multimedia*, 3173–3181.